Adhesion and Viability of Two Enterococcal Strains on Covalently Grafted Chitosan and Chitosan/κ-Carrageenan Multilayers

S. Bratskaya,*,† D. Marinin,† F. Simon,‡ A. Synytska,‡ S. Zschoche,‡ H. J. Busscher,§ D. Jager,§ and H. C. van der Mei§

Institute of Chemistry, Far East Department of Russian Academy of Sciences, 159, ave. 100-letiya Vladivostoka, Vladivostok 690022, Russia, Leibniz Institute of Polymer Research Dresden, Hohe Strasse 6, D-01069 Dresden, Germany, and Department of Biomedical Engineering University Medical Centre Groningen and University of Groningen, Antonius Deusinglaan 1, 9713 AV Groningen, The Netherlands

Received June 4, 2007; Revised Manuscript Received July 11, 2007

Chitosans are natural aminopolysaccharides, whose low cytotoxicity suggests their potential use for nonadhesive, antibacterial coatings on biomaterials implant surfaces. Here, the antiadhesive behavior and ability to kill bacteria upon adhesion ("contact killing") of chitosan coatings were evaluated for two strains of *Enterococcus faecalis*, isolated from clogged biliary stents. Chitosan coatings covalently grafted or applied as chitosan/κ-carrageenan multilayers were characterized by ellipsometry, scanning force microscopy (SFM), X-ray photoelectron spectroscopy (XPS), and electrokinetic measurements. Decreases in initial bacterial deposition rates and the number of bacteria adhering in a more advanced state of the adhesion process were observed on both types of modified surfaces, with more pronounced effects on highly hydrated multilayers. Adhesion of negatively charged enterococci was slightly enhanced on chitosan-terminated multilayers, but antibacterial effect was absent on κ-carrageenan-terminated multilayers. Thus, the efficacy of multilayers remains an interesting interplay between the promoting effect of cationically charged groups on adhesion of negatively charged bacteria and, on the other hand, their antibacterial effects.

1. Introduction

Despite significant progress achieved in the last decades, the prevention of bacterial adhesion and growth to biomaterials surfaces still remains one of the main challenges in the restoration of function in man using prosthetic implants. Bacterial adhesion and subsequent biofilm formation constitute a source of persistent infections that usually leads to the removal of the infected prosthesis.[1] Several antiadhesive and/or antibacterial coatings have been developed, based on hydrophobicing agents, application of positive charge, polymer brush coatings,[2,3] thermoresponsive polymers,[4] drug eluting coatings, silver coatings, natural[5,6] or synthetic polymeric biocides,[7,8] and many other developments. Yet, the clinical efficacies of many of these coatings still have to be demonstrated. Moreover, such coatings should not negatively impact tissue integration of a prosthesis, which eventually forms the best guarantee for the long-term functioning of an implanted prosthesis.[9]

Recently, a layer-by-layer technique based on alternating deposition of oppositely charged synthetic or natural polyelectrolytes has been proposed as a facile and affordable method to avoid a complicated multistage process of covalent grafting to yield materials with controllable adhesive properties.[10−12] Using weak, synthetic polyelectrolytes, Mendelsohn et al.[10] showed that, regardless of the constituent polymers, adjustment of pH and ionic strength during multilayer deposition provides a means to control biological interactions with the layers deposited. Elbert et al.[11] reported a monotonous decrease in the number of adhering fibroblasts with increasing number of deposited poly(L-lysine)/alginate multilayers on highly cell-adhesive gelatin-coated polystyrene surfaces.

Chitosan is a natural aminopolysaccharide (copolymer of β-(1−4) linked 2-acetamido-2-deoxy-D-glycopyranose and 2-amino-2-deoxy-D-glycopyranose) produced commercially by deacetylation of chitin from crustaceans exoskeletons and fungal cell walls. Sustainable interest in the biomedical application of chitosans to discourage bacterial adhesion and implant infection is stimulated strongly by the lack of toxicity of chitosans to mammalian cells[13] and its biodegradability[14] and strong antibacterial properties.[15] Covalent grafting of chitosan to chemically inert biomaterials surfaces is usually preceded by grafting of acrylic acid to γ-ray irradiated,[5] plasma,[16] or ozone[17] pretreated surfaces and has been applied to polypropylene,[18−20] poly(ethylene terephthalate),[6,16] and other polyester fibers.[5,21] However, Lin et al.[22] reported significant bacterial adhesion after chitosan application to the lumen of oxidized polyethylene tubing and attributed this to higher roughness and positive charge of chitosan-modified surfaces. Considering the known antibacterial properties of chitosan, these observations call for alternative application techniques with enhanced antiadhesive and antibacterial effects.

Although chitosan is often referred to as a highly biocompatible polymer, its suitability for blood-contacting applications is limited by its relatively high thrombogenic activity,[23] which can be circumvented by the incorporation of sulfate groups directly to the chitosan backbone[24] or using chitosan in combination with sulfonated poly(ethylene glycol),[25] heparin,[26,27] or dextran sulfate.[26] In addition, sulfated polysaccharides like

* Corresponding author. Phone/Fax: +7-4232-313583. E-mail.: sbratska@ich.dvo.ru.
† Far East Department of Russian Academy of Sciences.
‡ Leibniz Institute of Polymer Research Dresden.
§ University of Groningen.

10.1021/bm700620j CCC: $37.00
Published on Web 08/18/2007

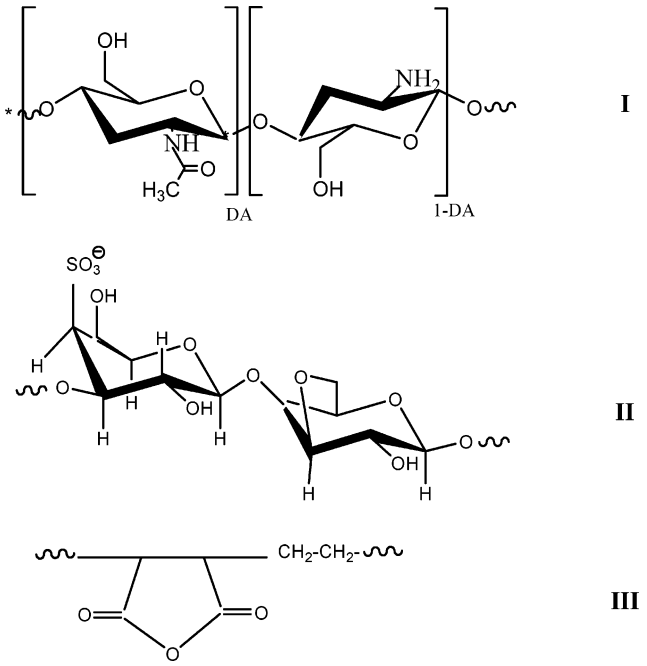

Figure 1. Chemical structure of the polyelectrolytes used for coatings preparation: I, chitosan (DA, deacetylation degree); II, κ-carrageenan; III, poly(ethylene-*alt*-maleic anhydride).

dextran sulfate can be used in the construction of multilayered coatings as described above.[28,29] Carrageenans provide a large family of natural, sulfated polysaccharides that are biocompatible, biodegradable, nontoxic, cheap, and gel-forming.[30] Recently, Schoeler et al.[31] showed that variation of carrageenan type for multilayers buildup allows formation of films differing in thickness, surface morphology, and elasticity, although the use of this class of polysaccharides to form coatings is limited hitherto.[31,32] Attempts to use carrageenans in developing antibacterial chitosan-containing coatings on biomaterials surfaces have never been made.

The aim of this paper is to compare the antibacterial efficacy of covalently grafted chitosan coatings with the efficacy of multilayers, consisting of chitosan and κ-carrageenan. Two aspects of antibacterial efficacy will be evaluated, i.e., the antiadhesive ability of the coatings as well as the ability of the coatings to kill bacteria upon adhesion ("contact killing"). Antibacterial efficacy will be determined against two clinically isolated strains of *Enterococcus faecalis*, an organism known to be involved in the clogging of biliary stents.

2. Experimental Section

2.1. Materials. Chitosan with a deacetylation degree of 84% and molecular weight of 3.4×10^5 g mol^{-1} was a gift from Pronova Biopolymers (Drammen, Norway). Poly(ethylene-*alt*-maleic anhydride), PEMAh, with molecular weight of 1.26×10^3 g mol^{-1} and κ-carrageenan (CAS 11114-20-8) were purchased from Aldrich and Fluka, respectively. Structures of the polymers are given in Figure 1. All other reagents were of analytical grade. Millipore water with a conductivity of <1 μS cm^{-1} was used in all experiments. Microscopic glass slides and highly polished single-crystal silicon wafers with a native SiO_2 layer of 1.8 ± 0.4 nm (Semiconductor Processing, Germany) were used as substrata for preparing coatings. Prior to polymer deposition, substrata were cleaned in $H_2O_2/NH_3/H_2O$ (1:1:1 v/v/v) mixture at 80 °C in an ultrasonic bath, thoroughly washed with distilled water, and dried at 120 °C.

2.2. Methods. *2.2.1. Multilayers Buildup.* Stock solutions of chitosans and κ-carrageenan with polymer content of 1 g L^{-1} were prepared in acetic acid (0.02 M) containing 0.15 M NaCl under constant stirring overnight (heating up to 50 °C was applied for the first 30 min). After filtration through cellulose filters with pore size of 0.45 μm, the pH of the polymer solutions was adjusted to pH 5 or pH 3, using 0.1 M NaOH or acetic acid. To avoid acidic degradation reported for κ-carrageenan,[33] only freshly prepared solutions were used for multilayers buildup. Multilayers were prepared by successive immersion of a substratum to solutions of chitosan and κ-carrageenan for 20 min with intermediate careful rinsing under running Millipore water. One layer of chitosan and one layer of κ-carrageenan are further referred to as a double layer.

2.2.2. Chitosan Grafting. Grafting of chitosan on glass surfaces and silicon wafers proceeded in three stages. In the first stage, the cleaned substrata were stored overnight in the presence of 3-aminopropyldimethylmono-ethoxysilane (100 μL in an extra small open Perti dishes). After drying the aminosilanized substrata at 120 °C for 1 h, a solution of PEMAh (0.03 g dissolved in a mixture of 6.66 g of acetone and 13.34 g of THF, filtered with 0.2 μm syringe filter) was spin-coated at 4000 rpm for 30 s. The coated samples were dried in vacuum at 120 °C for 2 h and thoroughly washed with acetone. Finally, chitosan solutions in 0.02 M acetic acid (0.4% w/v) with pH adjusted to 3 and 5 were spin-coated at 2000 rpm during 30 s. Modified slides (PEMAh−CH, pH 3 and PEMAh−CH, pH 5) were annealed at 120 °C for 2 h to yield covalent grafting and thoroughly washed.

2.2.3. Surface Topography. The multilayers topographies were investigated with a scanning force microscope (SFM) DI-3100 (Digital Instruments, Santa Barbara). The tapping mode was used to map the surface morphology at ambient conditions. Standard silicon tips with radius of about 10−30 nm, apex angle 65° were used at a frequency of about 275 kHz. From the height image, the root-mean-square (rms) roughness over the scan area of 1×1 μm^2 was calculated.

2.2.4. X-ray Photoelectron Spectroscopy (XPS). All XPS studies were carried out by means of an AXIS ULTRA photoelectron spectrometer (KRATOS ANALYTICAL, Manchester, England). The spectrometer was equipped with a monochromatic Al Kα ($h\nu = 1486.6$ eV) X-ray source of 300 W at 15 kV. The kinetic energy of photoelectrons was determined with a hemispheric analyzer set to pass energy of 160 eV for wide-scan spectra and 20 eV for high-resolution spectra, respectively. During all measurements, electrostatic charging of the sample was avoided by means of a low-energy electron source working in combination with a magnetic immersion lens. Later, all recorded peaks were shifted by the same value to set the C1s peak to 285.0 eV. Quantitative elemental compositions were determined from peak areas using experimentally determined sensitivity factors and the spectrometer transmission function. Spectrum background was subtracted according to Shirley.[34] The high-resolved spectra were deconvoluted by means of a computer routine. Free parameters of component peaks were their binding energy (BE), height, full width at half-maximum, and the Gaussian−Lorentzian ratio.

2.2.5. Electrokinetic Measurements. Electrokinetic properties of multilayers and coatings of covalently grafted chitosan layers were characterized by streaming potential measurements employing the Electrokinetic Analyzer EKA (Anton Paar GmbH, Austria) with a specially designed cell for plates and sheets.[35] For all samples, the electrolyte (KCl) concentration during measurements was 0.001 M. pH values were varied during measurements by the addition of 0.1 M HCl or 0.1 M KOH employing an automatic titration unit. ζ-Potential values were calculated from the experimentally determined streaming potential (dU/dp) according to the Smoluchowski equation.[36]

2.2.6. Ellipsometry. 2.2.6.1. Dry State Measurements. The thickness of polymer layers in the dry state was measured at $\lambda = 633$ nm and an angle of incidence of 70° with a null ellipsometer in a polarizer compensator sample analyzer (Multiscope, Optrel Berlin) microfocus ellipsometer. Initially, the thickness of the native SiO_2 layer was calculated at refractive indices $n = 3.858 - i(0.018)$ and $n = 1.4598$ for the Si wafer and the SiO_2 layer, respectively. The thickness of the PEMAh layer and chitosan/κ-carrageenan multilayers (ML) was evalu-

ated using the two-layer model Si/SiO_2/PEMAh(ML) with $n = 1.45$ and 1.5 for PEMAh and ML, respectively. The thickness of the chitosan layer (CH) was evaluated with the three-layer model Si/SiO_2/PEMAh/CH taking $n = 1.5$ for chitosan.[37] The measurements were averaged for at least 10 points for each sample.

2.2.6.2. "In Situ" Experiments. "In situ" ellipsometric measurements were performed to examine the swelling behavior of the chitosan/κ-carrageenan multilayers and PEMAh−CH layers in PBS (pH = 6.8, 0.15 M NaCl). An ellipsometric cell with thin glass walls, fixed at a known angle (68°) from the sample plane, was used. The angle of incidence of the light was set such that its path was normal to the window.

2.2.7. Bacterial Strains and Harvesting E. faecalis. BS385 and BS11297 clinical isolates from clogged biliary stents were used in this study. The strains were routinely cultured from frozen stock on blood agar plates. Precultures were inoculated with a single colony from plate in 3 mL of tryptone soya broth (TSB, Oxoid, Basingstoke, U.K.) and incubated overnight at 37 °C. Cultures were grown from the precultures in 200 mL of TSB overnight at 37 °C. Bacteria from overnight cultures were harvested by centrifugation (6500*g*, 5 min, 10 °C), washed twice, and resuspended in phosphate-buffered saline (PBS), pH 7.0 to a concentration of 3×10^8 cells mL^{-1}.

2.2.8. Bacterial Adhesion and Viability Assay. A parallel-plate flow chamber ($175 \times 17 \times 0.75$ mm^3) was used to monitor initial bacterial adhesion. Images were taken from the glass bottom plate, which contained the covalently grafted chitosan coating or chitosan/κ-carrageenan multilayers with 14 deposited double layers. The bacterial suspension flowed through the system at a volumetric flow rate of 0.023 mL s^{-1} (equivalent to a shear rate of 15 s^{-1}) for 1 h with recirculation at room temperature. The initial increase in number of adhering bacteria over time per unit area was expressed as the initial bacterial deposition rate, j_0, while the number of bacteria adhering after 1 h, denoted as N_{1h}, was taken as an estimate for adhesion at a more advanced state of the process. All adhesion experiments were preformed in triplicate with separately cultured bacteria.

After the adhesion experiments, flow was switched for 5 min to PBS without bacteria to remove unbound organisms from the tubes and the flow chamber at the same flow rate. The chamber was then filled with a solution of live/dead *bac*light bacterial viability stain (Molecular Probes, OR), to determine the percentage of viable, adhering bacteria, and from that moment was protected against light. After 30 min of staining, fluorescent images ($187.5\ \mu m \times 187.5\ \mu m$) were taken of each aliquot with a confocal laser scanning microscope (CLSM, Leica TCS SP2, Heidelberg, Germany). Bacteria were excited with 488 and 543 nm light, and emitted light with wavelengths of 495−535 nm, arising from viable bacteria, was assigned the color green, whereas the light from the 580−700 nm region, arising from nonviable bacteria, was assigned the color red. To prevent negative effects of the laser on bacterial viability, images were taken immediately after random image selection and never twice of the same area. Viability was defined as the percentage of viable bacteria relative to the total number of bacteria adhering. Aliquots taken from the entrance suspension were found to contain more than 95% viable organisms.

3. Results and Discussion

3.1. Covalently Grafted Chitosan Coatings. Grafting of acrylic acid to a solid substratum is often used as a preliminary stage of chitosan immobilization targeted to development of antibacterial coatings.[5,16,17,27] We applied PEMAh to graft chitosan to glass surfaces, since it is more reactive than poly(acrylic) acid due to the presence of anhydride groups. The film thickness in the dry state was 17 ± 0.5 nm, with equal contributions from PEMAh and chitosan. Taking into account the value of hydrodynamic radius (16−17 nm) for chitosan with comparable molecular weight and acetylation degree previously reported by Sorlier et al.,[38] we can assume that the chitosan coating thickness is close to that of chitosan monolayer. Figure 2 shows that coatings obtained at pH 3 are characterized by higher ζ-potentials and a shift in isoelectric point (IEP) toward higher pH values. This implies that the number of free amino groups on the surface is higher for the coatings obtained at pH 3 (PEMAh−CH, pH 3) than for those obtained at pH 5 (PEMAh−CH, pH 5).

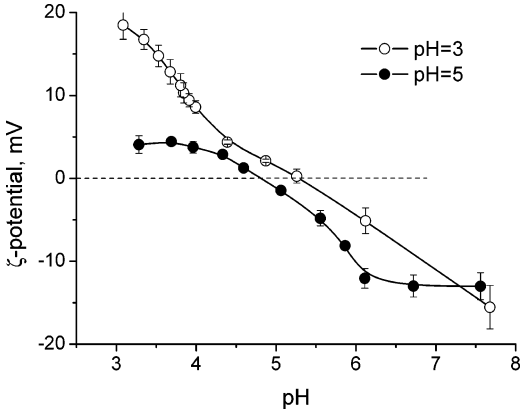

Figure 2. Electrokinetic properties of grafted chitosan coatings obtained at different pH values on glass, modified with PEMAh.

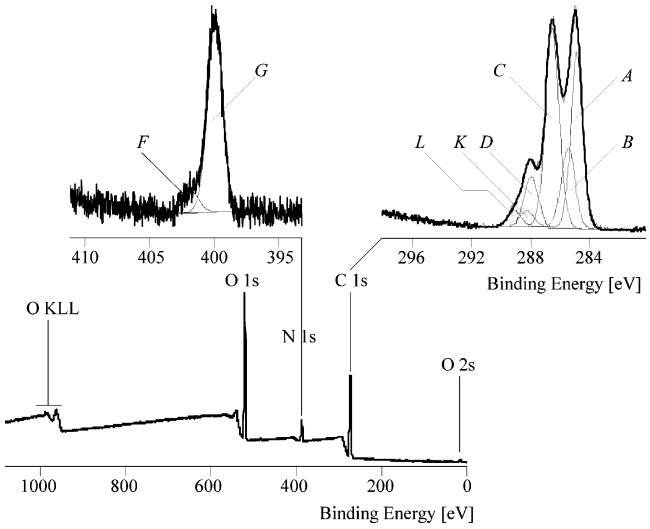

Figure 3. C 1s, N 1s, and survey spectra of covalently grafted chitosan layers (PEMAh−CH) obtained at pH 5.

XPS data supported the presence of a chitosan layer on top of the grafted PEMAh layer (Figure 3). The C 1s spectrum was deconvoluted to six component peaks (*A*, *B*, *C*, *D*, *K*, and *L*). Photoelectrons of saturated hydrocarbons (C_xH_y) from the PEMAh layer and minor surface impurities contributed to component peak *A* (285.0 eV), peaks *C* (286.8 eV) and *D* (287.9 eV) appeared from the *C*−OH and O−*C*−O groups of the saccharide unit, respectively. Peaks *K* (288.1 eV) and *L* (289.1 eV) were attributed to oxidized saccharide species and carbon in acetyl groups of residual chitinous units. Component peak B (285.9 eV) appeared from *C*−N bonds. The N 1s spectrum of PEMAh−CH, pH 5 was deconvoluted into two component peaks corresponding to the amino group *G* (399.5 eV) and protonated amino groups *F* (401.6 eV). The ratio of $[NH_3^+]/[NH_2]$ equal to 0.193 confirms, in accordance with the electrokinetic data, that the majority of the chitosan functional groups are in a deprotonated state. As we will show further, this ratio is in contrast with the state of the chitosan functional groups in multilayers (see Table 1), in which about 80% of the amino groups remained in a protonated state.

Table 1. Elemental Surface Concentration Ratios for Chitosan (CH*x*)/*κ*-Carrageenan (CAR*y*) Multilayers on Silicon Wafers after Different Numbers of Deposition Steps (DL)[a]

	CH3/CAR3				CH5/CAR3			
DL no.	2	6	8	12	2	6	8	12
N/C	0.129	0.083	0.061	0.064	0.173	0.097	0.061	0.062
S/C	0.145	0.063	0.048	0.051	0.180	0.087	0.058	0.059
N/S	0.89	1.317	1.271	1.255	0.961	1.115	1.052	1.051
$[NH_2]/[NH_3^+]$	0.242	0.226	0.303	0.186	0.358	0.133	0.357	0.268

[a] *x* and *y* denote the pH during chitosan or carrageenan deposition.

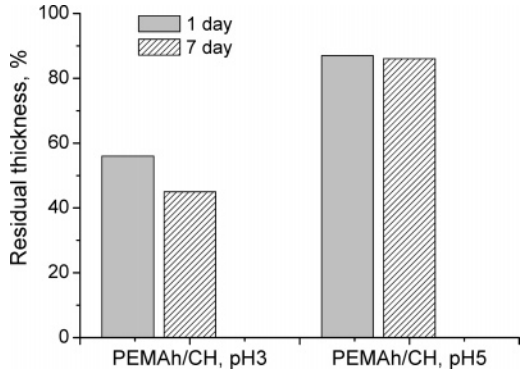

Figure 4. Stability of covalently grafted chitosan layers (PEMAh−CH) obtained at pH 3 and 5 in PBS (pH = 6.8, 0.15 M NaCl).

The swelling degree of PEMAh−CH coatings was rather low. The increase in film thickness upon immersion in PBS was 122% and 113% for PEMAh−CH, pH 3 and PEMAh−CH, pH 5, respectively. Stability of the coatings in PBS buffer was also different for these samples (Figure 4). Taking into account that a pH above 4 yields favorable conditions for acylation of chitosan with anhydrides of carbonic acids,[39] we suggest that amide bond formation was more efficient for PEMAh−CH, pH 5 ensuring higher cross-linking between polymers and better stability of the coatings. Lower ζ-potential and lower swelling degree of PEMAh−CH, pH 5, which was shown to be dependent on cross-linking for chitosan/poly(acrylic acid) complexes,[40] support this assumption.

3.2. Buildup of Chitosan/κ-Carrageenan Multilayers. *3.2.1. Growth of Chitosan/κ-Carrageenan Multilayers.* The pH-dependent charge density of chitosan ($pK_a = 6.2-6.5$[41]) enabled us to use pH alteration during polymer deposition as a convenient tool to control the thickness and structure of growing chitosan/*κ*-carrageenan multilayers. The original idea was to adsorb chitosan at two pH conditions corresponding to different conformational states (i) stretched, with fully charged amino groups (pH < 4), and (ii) more coiled, with partially deprotonated amino groups (e.g., pH = pK_a). In preliminary experiments, we found that chitosan adsorption on SiO_2 surfaces increased with increasing pH to reach a maximum at pH 6, but adsorption was reversible upon exposure of the chitosan-coated substratum to buffer. For this reason it was decided to decrease the pH at which the multilayers are formed, and here we report for pH 3 and 5.

Dry state ellipsometry measurements showed a noticeable difference in the thickness of the first adsorbed chitosan layer − 0.31 ± 0.04 to 0.86 ± 0.19 nm at pH 3 and 5, respectively. This clearly demonstrates that the growth of chitosan/*κ*-carrageenan multilayers can be controlled by pH adjustment. Figure 5 shows that chitosan/*κ*-carrageenan multilayers exhibit exponential growth with pH-dependent thickness increments per double layer. This type of growth was previously reported for polysaccharide-containing multilayers, and a possible mechanism of exponential growth was discussed.[12] The slowest film growth was observed when both chitosan and *κ*-carrageenan were adsorbed from solutions at pH 3 (CH3/CAR3). Increase of the deposition pH up to 5 (CH5/CAR5), significantly promoted film growth, but the highest thickness increment was achieved when the pH of the deposition solution was periodically changed during multilayers buildup from pH 5 for chitosan to pH 3 for *κ*-carrageenan (CH5/CAR3).

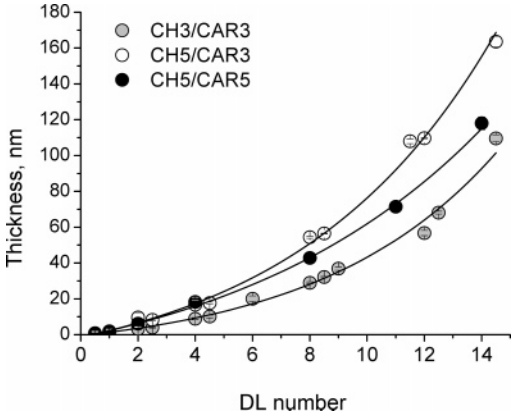

Figure 5. Dependence of the thickness (TH) of chitosan (CH*x*)/*κ*-carrageenan (CAR*y*) multilayers (dry state) on the number of deposited double layers (DL). *x* and *y* denote the pH during chitosan or carrageenan deposition. Data were fitted with the exponential growth function $TH = A \exp(DL/t) + B$, where $A = 11.08 \pm 0.48$, $t = 6.25 \pm 0.13$, $B = 11.70 \pm 0.51$ for CH3/CAR3; $A = 30.62 \pm 3.12$, $t = 8.92 \pm 0.54$, $B = -32 \pm 3$ for CH5/CAR5; $A = 24.35 \pm 0.59$, $t = 6.97 \pm 0.08$, $B = -25.78 \pm 0.69$ for CH5/CAR3.

The fast initial growth of CH5/CAR5 multilayers as compared to CH3/CAR3 is due to a higher amount of chitosan deposited in the first layer at pH 5 and, therefore, required a higher amount of *κ*-carrageenan to allow charge compensation (Figure 5). The accelerated further growth of CH5/CAR3 is most likely related with successive changes in ionization state of chitosan during multilayers buildup. Considering the pK_a value of chitosan, a 10% increase in fraction of protonated amino groups can be expected when pH is shifted from 5 to 3. Good permeability of multilayers to protons[42] allows an increase of surface charge when a chitosan-terminated multilayer is immersed into the *κ*-carrageenan solution at pH 3. Hence, for the same amount of chitosan as adsorbed in the CH5/CAR5 system, a higher amount of *κ*-carrageenan should be adsorbed to compensate for the additional positive charge. Due to the small difference in ionization state of chitosan at pH 3 and 5, the accelerated growth of the film thickness induced by this pH shift is within the experimental error for the first four double layers of CH5/CAR5 and CH5/CAR3 (see Figure 5). However, it becomes significant with increasing number of deposition steps due to the exponential type of growth of chitosan/*κ*-carrageenan multilayers. Thus it appears that minor, pH-induced changes in charge density of chitosan during multilayers buildup can promote growth of the film to obtain the desired thickness at reduced number of deposition steps. Further characterization of the multilayers is focused on two extreme cases—CH3/CAR3 and CH5/CAR3.

3.2.2. Electrokinetic Properties. Streaming potential measurements are often used to monitor the evolution of the surface charge during multilayers buildup.[43,44] When both the substratum and the adsorbing polyelectrolytes have high charge densities, adsorption of the first polymeric layer leads to charge reversal of the modified surface, close to the one of the polymer in solution[44] or somewhat lower.[45] Further adsorption of consecu-

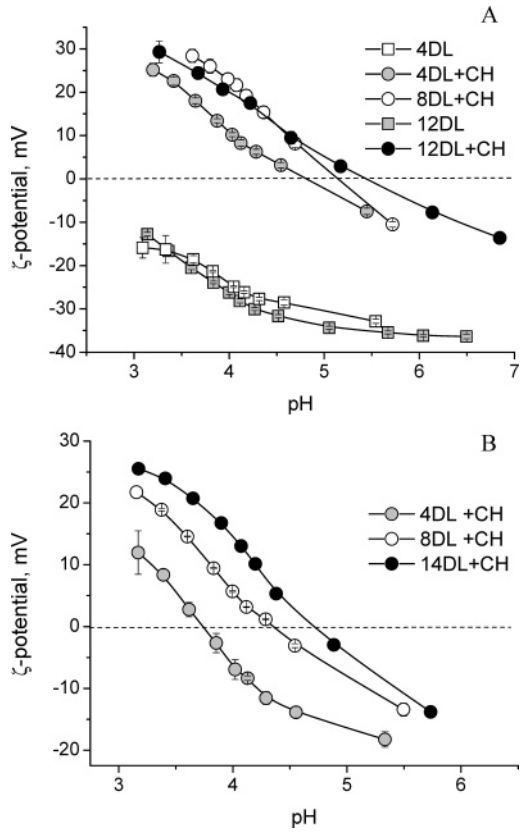

Figure 6. Electrokinetic properties of multilayers of chitosan (CH*x*)/*κ*-carrageenan (CAR*y*) multilayers as a function of pH. *x* and *y* denote the pH during chitosan or carrageenan deposition: (A) CH5/CAR3, (B) CH3/CAR3.

tive polyelectrolyte layers typically results in periodic oscillation of the ζ-potential[44] with a possible decrease in amplitude after deposition of a significant number of double layers.[43]

Unlike most previously reported multilayers systems formed by different polyelectrolyte pairs buildup at medium and high ionic strength, adsorption of the first chitosan layer from 0.15 M NaCl solution at pH = 3−5 did not raise the ζ-potential of the glass slides to values close to those of chitosan in solution (+40 mV), and the surface IEP was also significantly lower than expected at complete surface coverage by polycations with a pK_a of about 6. Nevertheless, the resulting surface properties were significantly different from those of the bare substratum, and the IEP of the surface was shifted to pH 3.3 and pH 4 for chitosan layers adsorbed from solutions at pH 3 and 5, respectively.

Figure 6 shows a significant difference in the evolution of the ζ-potential for multilayers assembled at different pH conditions. The effect of the underlying substratum for CH5/CAR3 is limited to four double layers, whereas it extends to at least eight double layers for CH3/CAR3. A further increase in the number of deposited double layers results in periodic oscillations of ζ-potentials, typical for multilayered systems. It should be noted that even at complete surface coverage, the ζ-potential of the chitosan-terminated layer is still lower than the ζ-potential of chitosan in solution. The IEP of the multilayered systems range between pH 5 and 5.5, possibly indicating a contribution of the sulfo groups of *κ*-carrageenan. The pH dependence of the ζ-potentials of *κ*-carrageenan-terminated multilayers (Figure 6A) can be accounted for similar effects of the chitosan amino groups on the final surface properties due to high degree of polymers interpenetration within the double layer.

3.2.3. SFM Imaging. SFM imaging was done to determine the morphology and surface roughness of the multilayers obtained at different pH and for a different number of deposition steps. The surface of the multilayers contains elongated structures whose length and thickness increase with increasing number of deposited layers, although the patterns become more fuzzy with an increase in the number of deposited layers (Figure 7). Note that phase imaging yielded sharper structural features than could be obtained in the height mode. Imaging of the surface of two double layers terminated with chitosan (CH3/CAR3) shows that the polyelectrolyte complexes are organized into a network of wormlike structures, which are 80−100 nm long and have nodules with a diameter of about 20 nm over the full length. The surface pattern of CH5/CAR3 at the same number of deposited layers was very similar (data not shown), but the surface coverage was visibly higher and the size of nodules varied in broader range. The rms roughness of the multilayers formed under periodically varying pH conditions (CH5/CH3) was notably higher than when formed at constant pH 3 (CH3/CAR3) −12.18 ± 0.85 and 7.29 ± 0.17 nm, respectively.

3.2.4. XPS. All coatings showed similar C 1s spectra (Figure 8) regardless of the mode of deposition, typical for polysaccharides and containing six component peaks (*A*, *B*, *C*, *D*, X1, and X2). Photoelectrons of saturated hydrocarbons (C_xH_y) contribute to component peak *A* (285.0 eV). Since the employed polysaccharides do not possess any saturated hydrocarbons, peak A must be attributed to carbon contamination, common for all surfaces. The two peaks *C* (286.8 eV) and *D* (287.9 eV) appear from the *C*−OH and O−*C*−O groups of the saccharide unit, respectively, and their ratio is in agreement with their stoichiometric ratio in chitin ($[D]/[C]|_{stoi,chitin} = 0.25$) and carrageenan ($[D]/[C]|_{stoi,car} = 0.2$). Two further component peaks X1 (288.1 eV) and X2 (289.1 eV) contribute to the C 1s spectra and are due to oxidized saccharide species (e.g., keto and *C*OOH groups) and nonhydrolyzed chitin species −C−NH−*C*═O, respectively. All samples show a pronounced component peak *B* at 285.9 eV. Its origin is the *C*−N bond of the chitosan's amine groups and the residual amide groups −*C*−NH−C═O−.

The S 2p spectra are composed of S $2p_{3/2}$ and S $2p_{1/2}$ peaks (Figure 8), both of each represent sulfur in its highest oxidation state, i.e., sulfate −O−*S*O_3^-. The N 1s spectra (Figure 8) show the presence of two component peaks indicating amine C−*N*H_2 or/and amide nitrogen C−*N*H−C═O (component peak F) and protonated amine (ammonium) species C−NH_3^+ (component peak G). Interestingly, ammonium species clearly dominate in the present coatings, demonstrating that the combination of chitosan with a strong polyelectrolyte as carrageen results in a permanent protonation of the amino groups in chitosan. Obviously, the completely dissociated sulfate groups of carrageenan stabilize the ammonium ions (−O−SO_3^-···H_3^+N−) and prevent the proton donation as well as the charge neutralization by simple electrolyte anions.

Table 1 shows that the surface chemistry is independent of the number of deposited double layers, and although two double layers do not fully cover the substratum surface, formation of −O−SO_3^-···H_3^+N− ion pairs is clearly indicated. Stoichiometry of polyelectrolytes interaction in multilayers accessed via calculation of N/S ratio was close to 1:1 for the system CH5/CAR3, whereas for the system CH3/CAR3, the N/S the ratio was close to unity only for 2 DL (double layers) (Table 1). Evidently, deviations from charge stoichiometry during complex formation are typical for pairs of polyelectrolytes differing in charge density,[46] among others due to a mismatch in intercharge

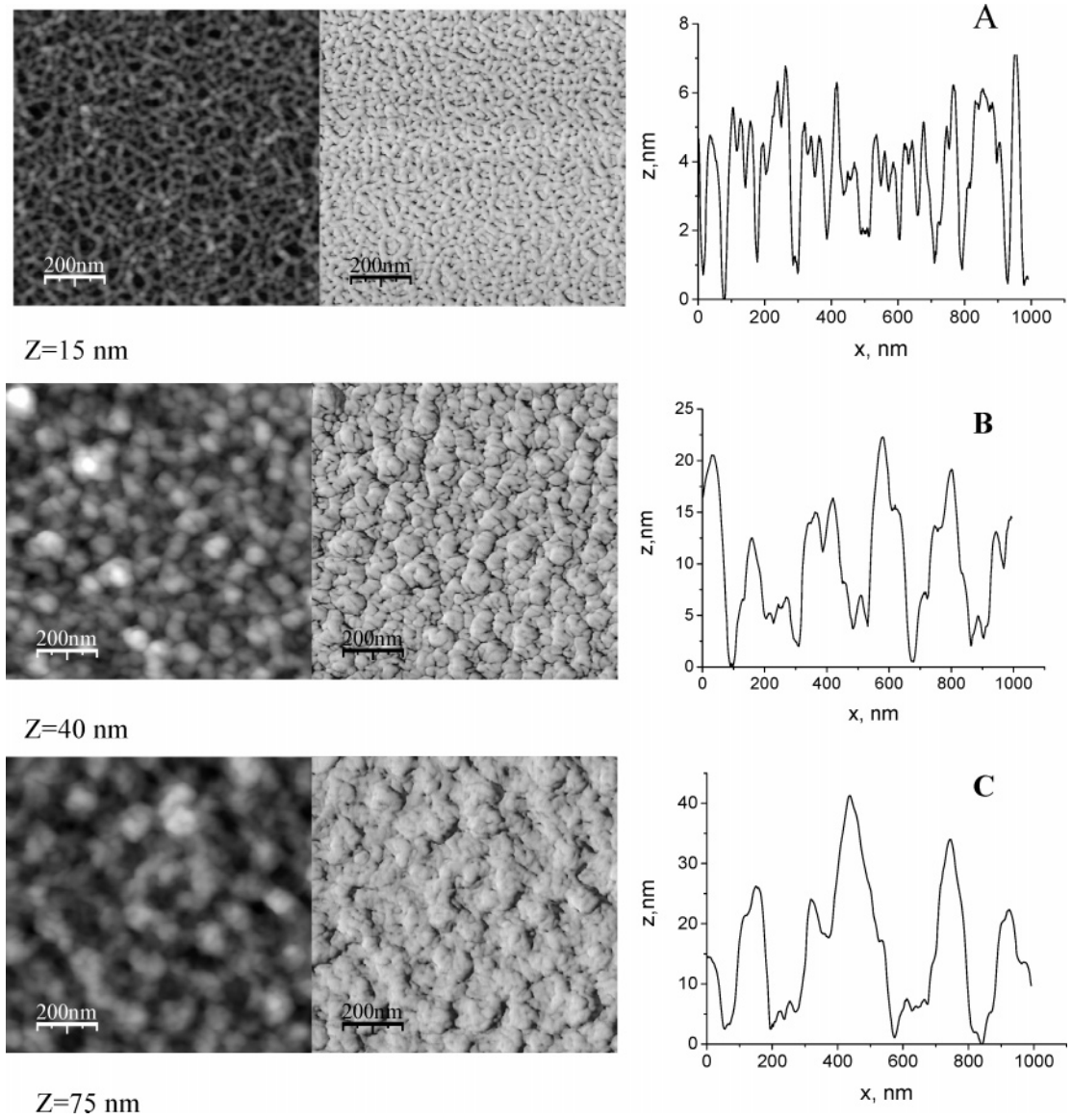

Figure 7. Representative SFM images (from left to right, height mode, phase mode, cross section) of chitosan/κ-carrageenan multilayers formed at pH 3 and terminated with chitosan (CH3/CAR3): (A) 2 DL (double layers), (B) 8 DL, (C) 12 DL.

distance for chitosan and κ-carrageenan (approximately every second saccharide unit of κ-carrageenan is uncharged, see Figure 1).

The fact that the stoichiometry of chitosan/carrageenan polyelectrolyte complexes formed in solution was close to unity[33] does not imply that this correlation should hold for the surface complexes, when interactions are strongly vectored by conformation of the first adsorbed polymer layer. Results of ellipsometry, electrokinetic measurements, and SFM show that chitosan adsorbed at pH 3 forms a very thin layer assuming complete coverage by a stretched conformation of fully ionized polyelectrolyte and strong segment−surface interactions. The thickness increment per double layer is also significantly lower for CH3/CAR3 than for CH3/CAR5. Thus, complex formation in the former case occurs in more confined conditions when the lack of conformational freedom of adsorbed polymer does not allow one-to-one pairing of charged groups as possible in solution. Bulky uncharged units of κ-carrageenan can screen amino groups of chitosan before the surface charge neutralization is reached. As a result, CH3/CAR3 multilayers can have excessive content of chitosan.

3.2.5. Swelling and Stability in PBS Buffer. The importance of swelling and hydration of the polymeric films for their interactions with living cells was emphasized by several research groups.[10,12,47] Regardless of preparation conditions, ellipsometrically measured thicknesses of chitosan/κ-carrageenan multilayers increased in PBS buffer up to 150% that implies higher hydrophility of multilayered coatings as compared to covalently grafted chitosan layers. Although it was also attempted to determine the kinetics of swelling by "in situ" ellipsometry, swelling occurred too fast in comparison with the time required to align the ellipsometer. Nevertheless, on the basis of these experiments, it can be concluded that bacterial adhesion was carried out (see section 3.3) on completely swollen multilayers.

After 7 days of immersion of the multilayers in PBS, no significant changes in film thickness were demonstrated by ellipsometry on dried films. Such high stability is typical for polyelectrolyte multilayers due to the strong electrostatic interactions of the constituent components in the film[48,49] and has also been observed at physiological temperature.[49]

3.3. Antiadhesive and Antibacterial Properties of Chitosan-Containing Coatings. The majority of studies on antibacte-

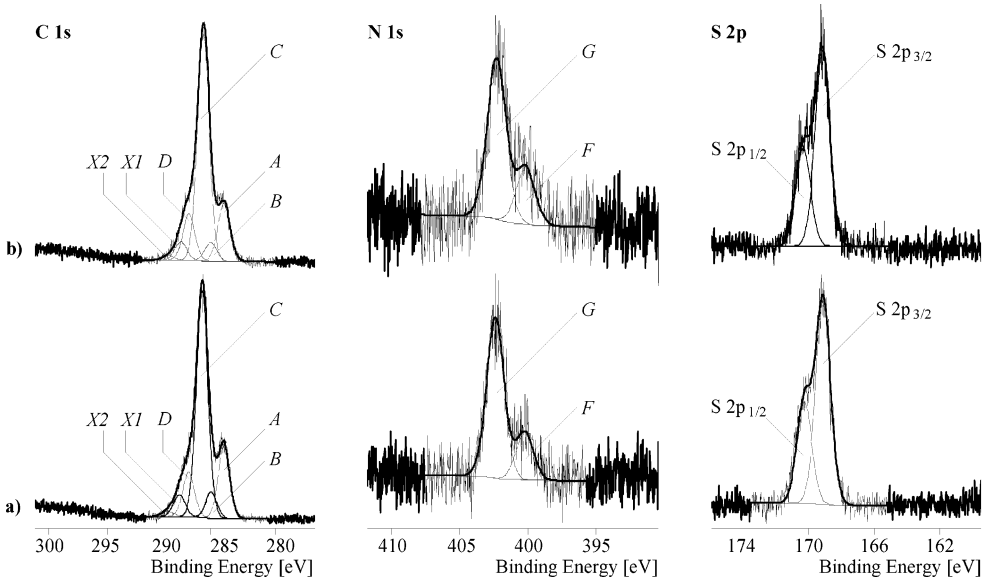

Figure 8. C 1s, N 1s, and S 2p XPS spectra of chitosan (CH*x*)/*κ*-carrageenan (CAR*y*) multilayers (8 DL) prepared onto silicon wafer substrates: CH3/CAR3 (a), CH5/CAR3 (b). *x* and *y* denote the pH during chitosan or carrageenan deposition.

rial properties of polymers and fibers grafted with chitosan were performed in suspension, where the viability of planktonic bacteria is evaluated as a function of the immersion time of the modified substratum in the suspension. Typically, changes in dead/live ratio of the planktonic bacteria in suspension were observed after 2−3 h of immersion.[6,16,18] Suspension testing of biomaterials coatings, however, is highly inappropriate for several reasons. First, infection of implants is a surface associated problem and bacteria in a biofilm mode of growth may both phenotypically as well as genotypically differ from their planktonic counterparts in suspension. Second, suspension testing relies on the release of chitosan during immersion, which leaves the surface of the implant unprotected. Moreover, our coating efforts were aimed at irreversibility. Therefore, we studied the efficacy of the coatings in terms of antiadhesivity and killing upon contact. Choice of two clinically isolated strains of *E. faecalis* (BS11297 and BS385) for evaluation of antiadhesive and antibacterial properties of chitosan-based coatings was determined by a high relevance of these strains in clogging of biliary stents. Prevention of biofilm formation and subsequent clogging of stents requires development of a surface modification strategy which, first of all, minimizes bacterial adhesion and, preferably, reduces bacterial viability at the surface. Although chitosan is often claimed to be a polymer with good antibacterial properties, it shows very high strain selectivity with minimum growth inhibitory concentrations varying within 2 orders of magnitude.[15] We have previously reported that the two enterococcal strains involved in this study differed in cell surface charge and show different ability to adhere to a negatively charged surface.[50] Thus, it is important to compare how coating of the surface with chitosan or chitosan/*κ*-carrageenan multilayers affect adhesion behavior and viability of both strains.

Table 2 demonstrates that all chitosan coatings prepared yielded significant decreases in initial bacterial deposition rates as well as in the number of bacteria adhering in a more advanced state of the adhesion process as compared with uncoated glass ($p < 0.01$, Student *t* test). These decreases are generally much (1−2 log units) larger than observed for hydrophobic or other coatings and approach those found for polymer brushes,[3] which suggests, considering the different chemistries involved in both types of coatings, that these reductions in bacterial adhesion must be attributed to the highly hydrated state of both PEO-polymer brushes and the present chitosan coatings. It should be noted that these extremely low numbers of adhering bacteria on the chitosan coatings cause large standard deviations in microscopic enumeration, as applied here. Since the microscopic field of view is already maximized and cannot be further increased due to the magnification required for visualization of bacteria, only 10−20 bacteria are actually counted in one field of view for chitosan-coated substrata.

Although there were no significant differences in antiadhesive performance between the differently terminated multilayers, nor between the two different covalently grafted layers, the antiadhesive performance of covalently grafted chitosan layers (PEMAh−CH) in general was worse than that of chitosan/*κ*-carrageenan multilayers independently on pH of chitosan deposition. Statistical analyses over the averaged data for the different multilayers and grafted layers demonstrate that the multilayers are significantly less adhesive than grafted layers ($p < 0.01$, Student *t* test). At the same time, average viabilities of adhering *E. faecalis* BS385 and *E. faecalis* BS11297 were lower ($p < 0.001$ and $p < 0.05$, respectively, Student *t* test) for grafted PEMAh−CH coatings than for chitosan-terminated multilayers and for both strains always significantly reduced with respect to glass ($p < 0.01$, Student *t* test). Taking into account the previous findings,[10,47] we suggest that the lower swelling degree of grafted chitosan layers was the main reason for the higher bacterial deposition rates on these substrata.

The initial bacterial deposition rates of both strains on CH5/CAR3 are somewhat higher than on CH3/CAR3 multilayers, which may relate with higher surface roughness of the former multilayers, since surfaces with lower roughness generally exhibit lower adhesivity.[51] Although variation of pH during multilayers buildup allowed control of the thickness increment per double layer, it influenced neither swelling behavior nor the initial bacterial deposition rates of the strains. Likely the initial bacterial deposition rates are more strongly controlled by the nature of the terminating polymer, although literature data are somewhat conflicting on this point. Hyaluronan-terminated chitosan/hyaluronan multilayers yielded adhesion of *Escherichiae coli* dependent on the nature of the terminating polymer,[12] but adhesion of NR6WT fibroblasts on polycation- and polyanion-terminated multilayers[10] was independent of the

Table 2. Adhesion of *E. faecalis* Strains (j_0 Is the Initial Bacterial Deposition Rate and N_{1h} Represents the Number of Adhering Bacteria after 1 h) and Their Viability on Multilayers of Chitosan (CH*x*)/κ-Carrageenan (CAR*y*) and Surface-Grafted Chitosans PEMAh−CH[a]

	E. faecalis BS385			*E. faecalis* BS11297		
	j_0 1/cm^2 s	N_{1h} 10^6/cm^2	viability %	j_0 1/cm^2 s	N_{1h} 10^6/cm^2	viability %
			Multilayers			
CH3/CAR3 chitosan-terminated	36 ± 21[b]	0.06 ± 0.03[b]	88 ± 5	45 ± 10[b]	0.12 ± 0.04[b]	79 ± 13
CH3/CAR3 carrageenan-terminated	17 ± 1[b]	0.04 ± 0.02[b]	92 ± 8	26 ± 4[b]	0.08 ± 0.04[b]	92 ± 3
CH5/CAR3 chitosan-terminated	115 ± 67[b]	0.11 ± 0.09[b]	89 ± 4	63 ± 33[b]	0.13 ± 0.06[b]	85 ± 8
CH5/CAR3 carrageenan-terminated	56 ± 35[b]	0.07 ± 0.03[b]	86 ± 10	25 ± 7[b]	0.07 ± 0.03[b]	96 ± 2
average for multilayers	59 ± 56[c]	0.07 ± 0.06[c]	87 ± 7[c]	40 ± 23[c]	0.10 ± 0.04[c]	88 ± 10
			Covalently Grafted Layers			
PEMAh−CH, pH = 3	149 ± 75[b]	0.31 ± 0.43[b]	73 ± 9[b]	296 ± 133[b]	0.15 ± 0.03[b]	78 ± 15
PEMAh−CH, pH = 5	183 ± 109[b]	0.30 ± 0.03[b]	36 ± 22[b]	301 ± 137[b]	0.22 ± 0.07[b]	76 ± 3[b]
average for grafted layers	163 ± 84	0.31 ± 0.31	54 ± 25	298 ± 121	0.19 ± 0.06	77 ± 11
			Glass (Control)			
	1260 ± 333	3.57 ± 0.12	93 ± 5	1018 ± 336	0.93 ± 0.38	97 ± 2

[a] *x* and *y* denote the pH during chitosan or carrageenan deposition; ± represents the SD over triplicate experiments with separately prepared coatings and different bacterial cultures. [b] Significantly different from data on glass ($p < 0.01$, Student *t* test). [c] Significantly different from averages for grafted layers ($p < 0.01$, Student *t* test).

ionic nature of the terminating polymer. Our data show that the enterococcal initial deposition rate was about twice lower for κ-carrageenan-terminated than for chitosan-terminated multilayers (Table 2), which is most likely associated with a stronger electrostatic repulsion between negatively charged sulfo groups of κ-carrageenan and negatively charged bacterial cell surfaces.

Adhesion to highly hydrated surfaces may cause the adhering bacteria to remain in a more planktonic state and prevent transition to a more resistant biofilm mode of growth. κ-Carrageenan-terminated multilayers caused very little bacterial death, and the viability of the adhering bacteria was very close to the one found on glass (control). Oppositely, on chitosan-terminated multilayers, a higher proportion of dead bacteria was found after 1 h of contact. This implies that despite the often reported loss of chitosan antibacterial function with deprotonation of amino groups in solution at pH 6.5−7,[15] moderate antibacterial efficacy remains under physiological conditions, i.e., in PBS and at pH 7. Chitosan/κ-carrageen multilayers combine chitosan as a rather weak polyelectrolyte with the strong polyelectrolyte carrageenan. Under physiological conditions, the sulfo groups of carrageenan are completely dissociated and can form ion pairs $-O-SO_3^- \cdots H_3^+N-$ with amino groups of chitosan that can stabilize its cationic charge over broader pH range and contribute to its antibacterial activity at elevated pH values.

Therewith, the ultimate efficacy of our multilayers remains an interesting interplay between the promoting effect of the cationically charged groups on adhesion of negatively charged bacteria and on the other hand, their antibacterial effects.

4. Conclusions

In this paper, we have compared the antiadhesive and antibacterial properties of two types of chitosan-based coatings against strains of *E. faecalis*. Covalently grafted chitosan layers were prepared using a highly reactive copolymer of maleic acid anhydride. Multilayers were built up from chitosan and sulfopolysaccharide κ-carrageenan. Coatings differed in thickness (100−170 nm for multilayers and 17−18 nm for covalently grafted layers), morphology, swelling behavior, and surface chemistry.

Chitosan/κ-carrageenan multilayers exhibited an exponential type of growth with pH-dependent thickness increment per double layer. The thinner films of highly interpenetrated polymers were obtained when both polyelectrolytes were adsorbed at pH 3. Increase of deposition pH up to 5 accelerated film growth, but the highest thickness increment was achieved by changing the deposition pH from 5 down to 3 for chitosan and κ-carrageenan adsorption steps, respectively. Amino groups of chitosan in multilayers are predominately in a protonated state, confirming their strong ion pairing with sulfo groups of κ-carrageenan, in contrast to amino groups of covalently grafted chitosan, which were predominately in a deprotonated state.

Surface roughness increased with increasing number of deposited double layers and was higher for chitosan/κ-carrageenan multilayers formed under stepwise variation of pH (from pH 5 to pH 3). Decreases in initial adhesion rates as well as in the numbers of bacteria adhered after 1 h were observed on both types of chitosan coatings. However, the antiadhesive properties of multilayers were remarkably better compared to less hydrated, covalently grafted chitosan layers. The initial deposition rates of both *E. faecalis* strains were about twice lower on κ-carrageenan-terminated than on chitosan-terminated multilayers, while an antibacterial effect of the coatings was observed only in the latter case. Thus, highly hydrated chitosan/κ-carrageenan multilayers represent a promising system for development of antiadhesive coatings on biomaterials surface,

which are in addition bioinert or show mild antibacterial properties depending on the nature of terminating polymer.

Acknowledgment. Financial support from NATO under the Project CBP.NR.CLG 9820 12 and a Grant of the President of the Russian Federation (received by S.B.) are gratefully acknowledged. We thank also Dr. Simona Schwarz for providing laboratory space and access to the electrokinetic analyzer and C. Lehmann for preparation of PEMAh−CH coatings.

References and Notes

(1) Costerton, J. W.; Stewart, P. S.; Greenberg, E. P. *Science* **1999**, *284*, 1318−1322.
(2) Sharma, S.; Johnson, R. W.; Desai, T. A. *Langmuir* **2004**, *20*, 348−356.
(3) Roosjen, A.; Van der Mei, H. C.; Busscher, H. J.; Norde, W. *Langmuir* **2004**, *20*, 10949−10955.
(4) Yamato, M.; Konno, C.; Utsumi, M.; Kikuchi, A.; Okano, T. *Biomaterials* **2002**, *23*, 561−567.
(5) Hu, S. G.; Jou, C. H.; Yang, M. C. *J. Appl. Polym. Sci.* **2002**, *86*, 2977−2983.
(6) Li, P.; Wang, J.; Lu, W. C.; Sun, H.; Huang, N. *Key Eng. Mater.* **2005**, *288*−*289*, 331−334.
(7) Cen, L.; Neoh, K. G.; Kang, E. T. *Langmuir* **2003**, *19*, 10295−10303.
(8) Kanazawa, A.; Ikeda, T.; Endo, T. *J. Appl. Polym. Sci.* **1994**, *52*, 641−647.
(9) Gristina, A. G. *Science* **1987**, *237*, 1588−1595.
(10) Mendelsohn, J. D.; Yang, S. Y.; Hiller, J.; Hochbaum, A. I.; Rubner, M. F. *Biomacromolecules* **2003**, *4*, 96−106.
(11) Elbert, D. L.; Herbert, C. B.; Hubbell, J. A. *Langmuir* **1999**, *15*, 5355−5362.
(12) Richert, L.; Lavalle, P.; Payan, E.; Shu, X.; Prestwich, G.; Stoltz, J.; Schaaf, P.; Voegel, J.; Picart, C. *Langmuir* **2004**, *20*, 448−458.
(13) *Biochemistry of Antimicrobial Action*; Franklin, T. J., Snow, G. A., Eds.; Chapman & Hall: London, 1981.
(14) Lee, K. Y.; Ha, W. S.; Park, W. H. *Biomaterials* **1995**, *16*, 1211−1216.
(15) Rabea, E. I.; Badawy, M. E. T.; Stevens, C. V.; Smagghe, G.; Steurbaut, W. *Biomacromolecules* **2003**, *4*, 1457−1465.
(16) Huh, M. W.; Kang, I. K.; Lee, D. H.; Kim, W. S.; Park, L. S.; Min, K. E.; Seo, K. H. *J. Appl. Polym. Sci.* **2001**, *81*, 2769−2778.
(17) Hu, S. G.; Jou, C. H.; Yang, M. C. *J. Appl. Polym. Sci.* **2003**, *88*, 2797−2803.
(18) Yang, J. M.; Lin, H. T.; Wu, T. H.; Chen, C. C. *J. Appl. Polym. Sci.* **2003**, *90*, 1331−1336.
(19) Wang, C. C.; Chen, C. C. *J. Appl. Polym. Sci.* **2005**, *98*, 391−400.
(20) Liao, J. D.; Lin, S. P.; Wu, Y. T. *Biomacromolecules* **2005**, *6*, 392−399.
(21) Jou, C. H.; Lee, J. S.; Chou, W. L.; Yu, D. G.; Yang, M. C. *Polym. Adv. Technol.* **2005**, *16*, 821−826.
(22) Lin, C. H.; Lin, J. C.; Chen, C. Y.; Cheng, C. Y.; Lin, X. Z.; Wu, J. J. *J. Appl. Polym. Sci.* **2005**, *97*, 893−902.
(23) Okamoto, Y.; Yano, R.; Miyatake, K.; Tomohiro, I.; Shigemasa, Y.; Minami, S. *Carbohydr. Polym.* **2003**, *53*, 337−342.
(24) Lin, C. W.; Lin, J. C. *J. Biomater. Sci., Polym. Ed.* **2001**, *12*, 543−557.
(25) Amiji, M. M. *Carbohydr. Polym.***1997**, *32*, 193−199.
(26) Amiji, M. M. *J. Biomater. Sci., Polym. Ed.* **1996**, *8*, 281−298.
(27) Qu, X.; Wirsen, A.; Olander, B.; Albertsson, A. C. *Polym. Bull.* **2001**, *46*, 223−229.
(28) Fu, J. H.; Ji, J.; Yuan, W. Y.; Shen, J. C. *Biomaterials* **2005**, *26*, 6684−6692.
(29) Serizawa, T.; Yamaguchi, M.; Akashi, M. *Biomacromolecules* **2002**, *3*, 724−731.
(30) Richardson, R. K.; Goycoolea, F. M. *Carbohydr. Polym.* **1994**, *24*, 223−225.
(31) Schoeler, B.; Delorme, N.; Doench, I.; Sukhorukov, G. B.; Fery, A.; Glinel, K. *Biomacromolecules* **2006**, *7*, 2065−2071.
(32) Lee, S. S.; Lee, K. B.; Hong, J. D. *Langmuir* **2003**, *19*, 7592−7596.
(33) Hugerth, A.; Caram-Lelham, N.; Sundelof, L. O. *Carbohydr. Polym.* **1997**, *34*, 149−156.
(34) Shirley, D. A. *Phys. Rev. B* **1972**, *B5*, 4709−4714.
(35) Bellmann, C.; Klinger, C.; Opfermann, A.; Böhme, F. *Prog. Org. Coat.* **2002**, *44*, 93−98.
(36) Smoluchowski, M. *Handbook of Electrochemistry and Magnetism*; Barth: Leipzig, 1921; Vol. 2.
(37) Jiang, H.; Su, W.; Caracci, S.; Bunning, T. J.; Copper, T.; Adams, W. W. *J. Appl. Polym. Sci.* **1996**, *61*, 1163−1171.
(38) Sorlier, P.; Rochas, C.; Morfin, I.; Viton, C.; Domard, A. *Biomacromolecules* **2003**, *4*, 1034−1040.
(39) Satoh, T.; Vladimirov, L.; Johmen, M.; Sakairi, N. *Chem. Lett.* **2003**, *32*, 318−319.
(40) Nge, T. T.; Yamaguchi, M.; Hori, N.; Takemura, A.; Ono, H. *J. Appl. Polym. Sci.* **2002**, *83*, 1025−1035.
(41) Rinaudo, M.; Pavlov, G.; Desbrieres, J. *Polymer* **1999**, *40*, 7029−7032.
(42) Von Klitzing, R.; Möhwald, H. *Langmuir* **1995**, *11*, 3554−3559.
(43) Picart, C.; Lavalle, P.; Hubert, P.; Cuisinier, F. J. G.; Decher, G.; Schaaf, P.; Voegel, J. C. *Langmuir* **2001**, *17*, 7414−7424.
(44) Adamczyk, Z.; Zembala, M.; Warszynski, P.; Jachimska, B. *Langmuir* **2004**, *20*, 10517−10525.
(45) Ladam, G.; Schaad, P.; Voegel, J. C.; Schaaf, P.; Decher, G.; Cuisinier, F. *Langmuir* **2000**, *16*, 1249−1255.
(46) Chen, J. H.; Heitmann, J. A.; Hubbe, M. A. *Colloid Surf., A* **2003**, *223*, 215−230.
(47) Lo, C. M.; Wang, H. B.; Dembo, M.; Wang, Y. L. *Biophys. J.* **2000**, *79*, 144−152.
(48) Cai, K. Y.; Rechtenbach, A.; Hao, J. Y.; Bossert, J.; Jandt, K. D. *Biomaterials* **2005**, *26*, 5960−5971.
(49) Richert, L.; Boulmedais, F.; Lavalle, P.; Mutterer, J.; Ferreux, E.; Decher, G.; Schaaf, P.; Voegel, J.-C.; Picart, C. *Biomacromolecules* **2004**, *5*, 284−294.
(50) Van Merode, A. E. J.; Van der Mei, H. C.; Busscher, H. J.; Krom, B. P. *J. Bacteriol.* **2006**, *188*, 2421−2426.
(51) Lampin, M.; Warocquier-Clerout, R.; Legris, C.; Degrange, M.; Sigot-Luizard, M. F. *J. Biomed. Mater. Res.* **1997**, *36*, 99−108.

BM700620J